

# One-Dimensional Coordination Polymers Based on First-Row Transition Metals: A Solid-State Study of Weak Backbone Interactions

S. RUSSELL SEIDEL, FRANK M. TABELLION, ATTA M. ARIF, AND PETER J. STANG\*

Department of Chemistry, University of Utah, 315 S. 1400 E., Salt Lake City, Utah 84112, USA

(Received 14 October 2001)

**Abstract.** We present further data on the solid-state structures of one-dimensional coordination polymers based upon divalent transition metal hexafluoroacetylacetonate (hfacac) complexes. A variety of linking subunits are employed in order to investigate and probe the relatively weak interactions that make up the backbones of these polymers. Reported in this study are metal complexes containing manganese, zinc, copper, and cobalt and a range of donor building blocks encompassing an array of bonding motifs, including pyridyl–metal, pyridyl(*N*-oxide)–metal, and hydrogen bonding. The specific linkers utilized are 4,4'-dipyridyl *N,N'*-dioxide hydrate, 2,5-bis(4-ethynylpyridyl)furan, 4,4'-trimethylenedipyridine, and *trans*-1-(2-pyridyl)-2-(4-pyridyl)-ethylene. A detailed discussion of the products is presented, as is a comparison to known compounds of a similar nature. All compounds are characterized via single-crystal X-ray diffraction and elemental analysis for the bulk of the sample.

## INTRODUCTION

Over the past three to four decades, one-dimensional coordination polymers have been the focus of a significant amount of research.<sup>1</sup> Such species were among the predecessors and first members of the field that would later be termed “supramolecular self-assembly”, which can be broadly interpreted to encompass both solid-state phenomena, such as infinite network solids,<sup>2</sup> and solution-based phenomena, such as discrete molecular architecture.<sup>3</sup> In addition, coordination polymers have remained a subject of study in their own right with the discovery of an array of advantageous applications over the years.<sup>1b</sup> These potential uses include, but are not limited to, molecular magnets,<sup>4</sup> electrical conductivity and superconductivity,<sup>5</sup> non-linear optics,<sup>6</sup> and ferroelectric materials.<sup>7</sup>

With the recent interest in crystal engineering,<sup>2a,8</sup> the study of one-dimensional coordination polymers has taken on an additional facet. Generally speaking, the aim in this area is to be able to control the bulk properties of crystalline materials via fine-tuning the overall crystal topology. In order to do so, however, an in-

depth understanding of the wide variety of intra- and intermolecular interactions present in solid-state materials is required. Of relevance to the work presented here is our previous study of the reaction behavior of manganese(II) hexafluoroacetylacetonate trihydrate with 4,4'-trimethylenedipyridine,<sup>9</sup> wherein the resulting crystalline products could be tuned from closed dimeric macrocycles to helices and then to wedge-shaped syndiotactic polymers via simply changing the organic templates employed.

Herein, we continue our investigations into the solid-state structures of one-dimensional coordination polymers containing divalent transition metal hexafluoroacetylacetonate (hfacac) complexes in their backbones. Systems based on manganese, zinc, copper, and cobalt are explored, as the weak bonding motifs of the units linking them are varied and probed. These themes include pyridyl(*N*-oxide)–metal and pyridyl–metal dative bonding, as well as hydrogen bonding.

---

\*Author to whom correspondence should be addressed. E-mail: [stang@chem.utah.edu](mailto:stang@chem.utah.edu)

## EXPERIMENTAL

### Procedures

#### Preparation of $[Mn(hfacac)_2(4,4'-dipyridyl\ N,N'-dioxide)]_n$ (**3**)

When 37.8 mg (0.0723 mmole) of manganese(II) hexafluoroacetylacetonate trihydrate (**1**) is mixed with 15.4 mg (0.0818 mmole) of 4,4'-dipyridyl *N,N'*-dioxide hydrate (**2**) in an acetone–methanol solution, and slow evaporation of the solvent mixture is allowed to occur, 33.1 mg of (**3**) is produced (69.7%; red). Anal. Calcd for  $C_{20}H_{10}F_{12}MnN_2O_6$ : C 36.55, H 1.53, N 4.26%. Found: C 36.66, H 1.61, N 4.28%. X-ray quality crystals are grown from slow evaporation of a toluene–methanol solvent mixture.

#### Preparation of $[Zn(hfacac)_2(4,4'-dipyridyl\ N,N'-dioxide)]_n$ (**5**)

When 27.6 mg (0.0535 mmole) of zinc(II) hexafluoroacetylacetonate dihydrate (**4**) is mixed with 9.9 mg (0.0526 mmole) of 4,4'-dipyridyl *N,N'*-dioxide hydrate (**2**) in an acetone–methanol solution, and slow evaporation of the solvent mixture is allowed to occur, 21.8 mg of (**5**) is produced (62.2%; clear, faint yellow). Anal. Calcd for  $C_{20}H_{10}F_{12}N_2O_6Zn$ : C 35.98, H 1.51, N 4.20%. Found: C 36.12, H 1.41, N 4.21%. X-ray quality crystals are grown from slow evaporation of an acetone–methanol–toluene solvent mixture.

#### Preparation of $[Cu(hfacac)_2(7)]_n$ (**8**)

When 10.5 mg (0.0220 mmole) of copper(II) hexafluoroacetylacetonate hydrate (**6**) is mixed with 5.7 mg (0.0211 mmole) of 2,5-bis(4-ethynylpyridyl)furan (**7**) in an acetone–methanol solution, and slow evaporation of the solvent mixture is allowed to occur, 13.4 mg of (**8**) is produced (84.8%; green). Anal. Calcd for  $C_{28}H_{12}CuF_{12}N_2O_5$ : C 44.96, H 1.62, N 3.75%. Found: C 44.73, H 1.69, N 3.75%. X-ray quality crystals are grown from slow evaporation of an acetone–methanol solvent mixture.

#### Preparation of $[Mn(hfacac)_2(7)]_n \cdot 1.5 n(\text{benzene})$ (**10**)

When 10.0 mg (0.0191 mmole) of manganese(II) hexafluoroacetylacetonate trihydrate (**1**) is mixed with 5.2 mg (0.0192 mmole) of 2,5-bis(4-ethynylpyridyl)furan (**7**) in an acetone–methanol–benzene solution and slow evaporation of the solvent mixture is allowed to occur, 6.5 mg of (**10**) is produced (39.7%; yellow). Anal. Calcd for  $C_{28}H_{12}F_{12}MnN_2O_5$ : C 45.49, H 1.64, N 3.79%. Found: C 45.81, H 1.71, N 3.89%. X-ray quality crystals are grown from slow evaporation of an acetone–methanol–benzene solvent mixture.

#### Preparation of $[Co(hfacac)_2(12)]_n \cdot 0.5 n(N,N\text{-dimethylformamide})$ (**14**)

When 55.1 mg (0.116 mmole) of cobalt(II) hexafluoroacetylacetonate hydrate (**11**) is mixed with 22.7 mg (0.114 mmole) of 4,4'-trimethylenedipyridine (**12**) in an acetone–methanol–*N,N*-dimethylformamide solution and slow evaporation of the solvent mixture is allowed to occur, 43.9 mg of (**14**) is produced (54.4%; orange). Anal. Calcd for  $C_{49}H_{39}Co_2F_{24}N_5O_5$ : C 41.57, H 2.78, N 4.95%. Found: C 41.30, H 2.45, N 4.25%. X-ray quality crystals are grown from slow evaporation of an acetone–methanol–*N,N*-dimethylformamide solvent mixture.

#### Preparation of $\{[Mn(hfacac)_2(15)]_2\} \cdot [Mn(hfacac)_2(\text{MeOH})_2]_n$ (**16**)

When 101.4 mg (0.194 mmole) of manganese(II) hexafluoroacetylacetonate trihydrate (**1**) is mixed with 35.3 mg (0.194 mmole) of *trans*-1-(2-pyridyl)-2-(4-pyridyl)-ethylene (**15**) in an acetone–methanol solution and slow evaporation of the solvent mixture is allowed to occur, 99.5 mg of (**16**) is produced (75.3%; orange-yellow). Anal. Calcd for  $C_{22}H_{12}F_{12}MnN_2O_4$ : C 40.57, H 1.86, N 4.3%. Found: C 40.62, H 1.85, N 4.36%. X-ray quality crystals are grown from slow evaporation of an acetone–methanol solvent mixture.

### X-ray Crystallography

#### General Procedure

The crystals were mounted on a glass fiber with traces of viscous oil and then transferred to a Nonius KappaCCD diffractometer equipped with Mo  $K\alpha$  radiation ( $\lambda = 0.71073 \text{ \AA}$ ). Ten frames of data were collected at 200(1)K with an oscillation range of 1 deg/frame and an exposure time of 20 s/frame.<sup>10</sup> Indexing and unit cell refinement, based on all observed reflections from those ten frames, indicated the lattice type and space group. All reflections were indexed, integrated, and corrected for Lorentz, polarization, and absorption effects using DENZO-SMN and SCALEPAC.<sup>11</sup> Post refinement of the unit cell gave its final parameters, which were used in the final least-squares refinement of the structure. For the monoclinic systems, axial photographs and systematic absences were consistent with the compounds having crystallized in their respective space groups.

The structure was solved by a combination of direct methods and heavy atom using SIR 97.<sup>12</sup> All of the non-hydrogen atoms were refined with an anisotropic displacement coefficients. Hydrogen atoms were assigned isotropic displacement coefficients  $U(H) = 1.2U(C)$  or  $1.5U(C_{\text{methyl}})$ , and their coordinates were allowed to ride on their respective carbons using SHELXL97.<sup>13</sup> Scattering factors were taken from the International Tables for Crystallography, Vol. C.<sup>14,15</sup>

## RESULTS AND DISCUSSION

When equimolar amounts of manganese(II) hexafluoroacetylacetonate trihydrate **1** are reacted with 4,4'-dipyridyl *N,N'*-dioxide hydrate **2** in an acetone/methanol solution, the resulting solid-state product is that of coordination polymer **3** (Scheme 1).

The asymmetric unit of **3** shows a single metal-accepting unit and a single donor unit, with the linkages between them occurring through the *N*-oxide moiety of **2** (Fig. 1a). In addition, the overall shape adopted by **3** is that of a zig-zag polymer, which is a direct consequence of the nominally  $sp^3$  hybridization of the backbone oxygen atoms ( $Mn1-O5-N1 = 119^\circ$ ; Fig. 1b). The crystal packing diagram of **3** is as shown (Fig. 1c).

The coordination of the oxygen to the metal leads to a *trans*,  $180^\circ$  configuration of the ligands about each pseudo-octahedral manganese(II) center. This is con-

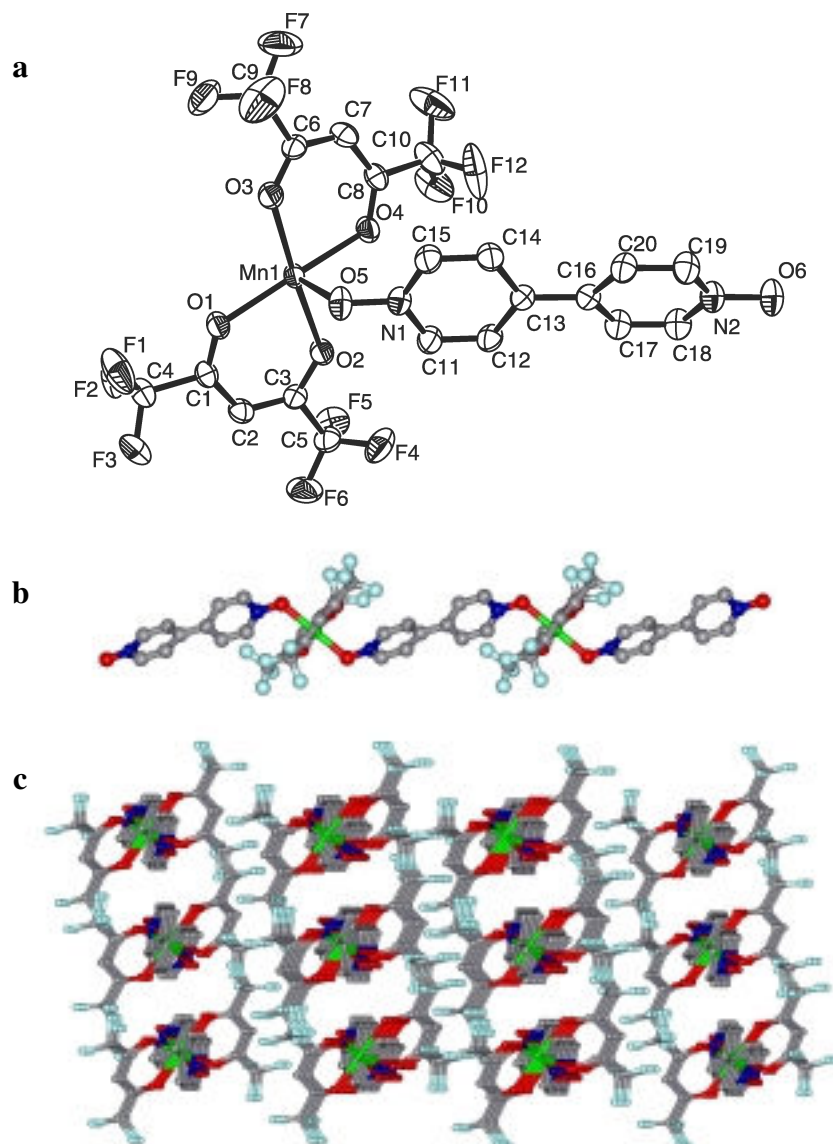
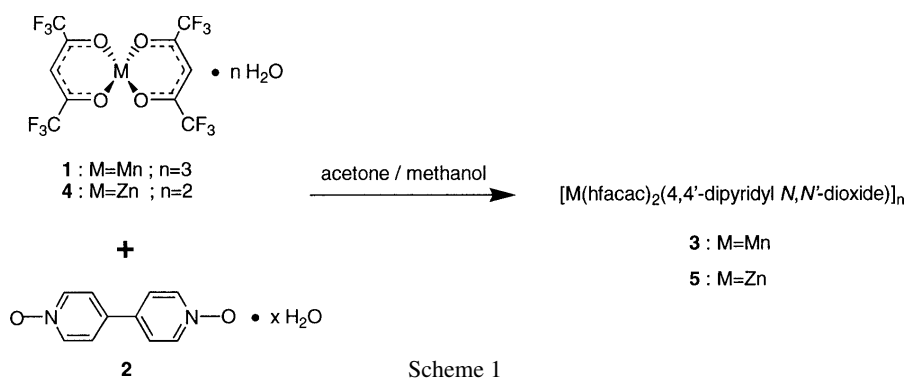


Fig. 1. (a) ORTEP plot of the asymmetric unit of **3** (protons omitted for clarity). (b) Portion of the polymeric chain of **3** (ball and stick representation; protons omitted for clarity). (c) Stacking diagram of **3** (ball and stick representation; protons omitted for clarity).

trary to our<sup>9</sup> and others<sup>16</sup> previous reactions of **1** involving pyridyl-bonding subunits, where a *cis*, 90° orientation is often, but not always,<sup>17</sup> achieved. This change in ligand arrangement does, however, allow for **3** to correspond well with copper and cobalt polymers of the same type found in the literature.<sup>16</sup>

When compared with the known, 4,4'-dipyridyl analogue,<sup>16</sup> which is also a zig-zag chain, **3** shows noteworthy differences. As noted above, the manganese centers present in the dipyridyl counterpart adopt the *cis* ligand orientation, as opposed to the *trans* seen for **3**. In addition, the Mn–O(*N*-oxide) bond distance in **3** is actually shorter (Mn1–O5 = 2.17 Å) than that seen for the comparable dipyridyl compound, where the Mn–N distance is 2.26 Å. This might indicate a stronger dative bond for the *N*-oxide-bound polymer. Other selected structural features are presented in Tables 1 and 2.

The reaction of zinc(II) hexafluoroacetylacetonate dihydrate **4** with 4,4'-dipyridyl *N,N'*-dioxide hydrate **2**, under conditions of formation similar to those of **3**, yields polymer **5** (Scheme 1). Similar to **3**, the asymmetric unit of **5** comprises one each of the acceptor and donor building blocks (Fig. 2). Again, by virtue of the nominal sp<sup>3</sup> hybridization of the backbone oxygen atoms that form the links between subunits **2** and **4**, a zig-zag coordination polymer arises (Zn1–O5–N1 = 118°).

Analogous to **3**, above, and similar, known copper and cobalt compounds,<sup>16</sup> a *trans*, 180° orientation of the ligands about the pseudo-octahedral zinc(II) centers is realized. As is also the case with **1**, subunit **4** has often exhibited a *cis*, 90° ligand arrangement when reacting with pyridyl donor units.<sup>1c,18</sup> The exact reason for these deviations is not entirely clear, but they do point to an interesting structural difference between the pyridyl and

Table 1. Crystallographic parameters for compounds **3** and **5**

|   | <b>3</b>  | <b>5</b>  |
|---|---|---|
| formula                                 | C <sub>20</sub> H <sub>10</sub> F <sub>12</sub> MnN <sub>2</sub> O <sub>6</sub> | C <sub>20</sub> H <sub>10</sub> F <sub>12</sub> ZnN <sub>2</sub> O <sub>6</sub> |
| <i>M</i>                                | 657.24  | 667.67  |
| <i>T</i> /K                             | 200(1)  | 200(1)  |
| system                                  | Monoclinic  | Monoclinic  |
| space group                             | <i>P</i> 2 <sub>1</sub> / <i>n</i>  | <i>P</i> 2 <sub>1</sub> / <i>n</i>  |
| <i>a</i> /Å                             | 10.8450(2)  | 10.9491(1)  |
| <i>b</i> /Å                             | 12.5101(4)  | 12.4011(3)  |
| <i>c</i> /Å                             | 17.6909(5)  | 17.4241(4)  |
| α°                                      | 90  | 90  |
| β°                                      | 99.1926(17)   | 100.3894(13)  |
| γ°                                      | 90  | 90  |
| <i>V</i> /Å <sup>3</sup>                | 2369.33(11)   | 2327.07(8)  |
| <i>Z</i>                                | 4   | 4   |
| μ/mm <sup>-1</sup>                      | 0.694   | 1.194   |
| <i>R</i> 1 ( <i>I</i> > 2σ( <i>I</i> )) | 0.0561  | 0.0475  |
| GOF                                     | 1.022   | 1.029   |

Table 2. Selected bond lengths [Å] and angles [°] for **3** and **5**

|                   |                   | Compound <b>3</b> |  | Compound <b>5</b> |            |
|-------------------|-------------------|-------------------|--|-------------------|------------|
| Bond lengths (Å)  | Mn(1)–O(4)        | 2.1470(19)        |  | Zn(1)–O(1)        | 2.0669(16) |
|                   | Mn(1)–O(1)        | 2.1479(19)        |  | Zn(1)–O(4)        | 2.0673(16) |
|                   | Mn(1)–O(2)        | 2.1482(18)        |  | Zn(1)–O(2)        | 2.0728(16) |
|                   | Mn(1)–O(3)        | 2.1525(18)        |  | Zn(1)–O(3)        | 2.0749(16) |
|                   | Mn(1)–O(5)        | 2.173(2)          |  | Zn(1)–O(5)        | 2.1038(18) |
|                   | Mn(1)–O(6)#1      | 2.184(2)          |  | Zn(1)–O(6)#1      | 2.1238(19) |
| Bond angles (deg) | O(1)–Mn(1)–O(2)   | 84.70(7)          |  | O(1)–Zn(1)–O(2)   | 88.93(6)   |
|                   | O(4)–Mn(1)–O(3)   | 84.76(7)          |  | O(4)–Zn(1)–O(3)   | 88.67(6)   |
|                   | N(1)–O(5)–Mn(1)   | 119.21(15)        |  | N(1)–O(5)–Zn(1)   | 118.30(13) |
|                   | N(2)–O(6)–Mn(1)#2 | 121.76(16)        |  | N(2)–O(6)–Zn(1)#2 | 121.05(14) |
|                   | O(5)–Mn(1)–O(6)#1 | 178.10(8)         |  | O(5)–Zn(1)–O(6)#1 | 178.44(7)  |

Symmetry transformations used to generate equivalent atoms: #1 *x*,*y*–1,*z*; #2 *x*,*y*+1,*z*.

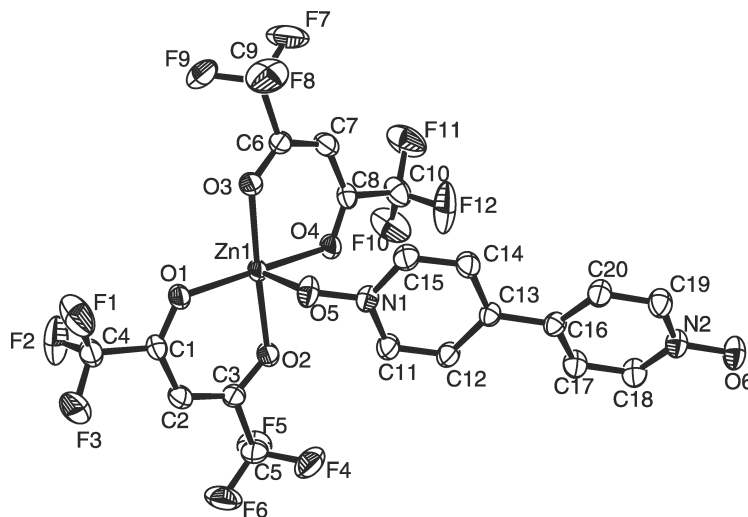


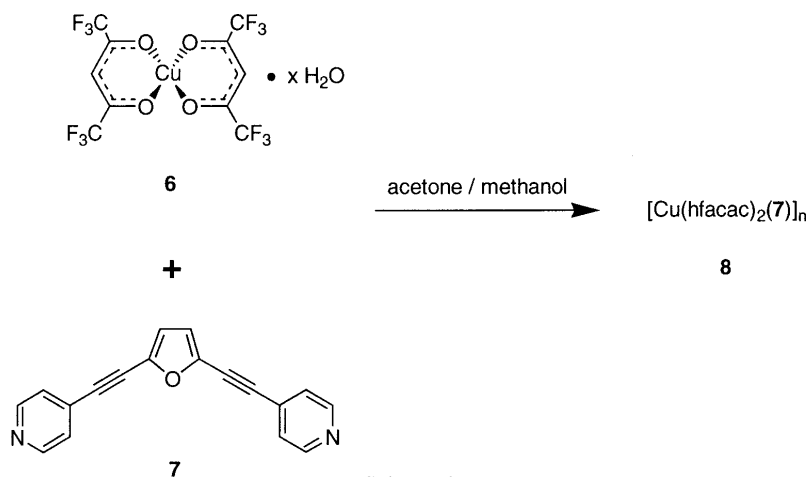
Fig. 2. ORTEP plot of the asymmetric unit of **5** (protons omitted for clarity).

*N*-oxide coordination chemistry of these two metal complexes. Furthermore, while the dative bonds of **3** are shorter than those of the corresponding dipyrindyl analogue, the Zn–O(*N*-oxide) linkages found for **5** (Zn1–O5 = 2.10 Å) are virtually identical to those of zinc pyridyl-based polymers found in the literature (Zn–N(pyridyl) = 2.10–2.12 Å).<sup>1c</sup> Finally, both polymers **3** and **5** show similar out-of-plane twists in the dipyrindyl portions of their backbones, with torsion angles C14–C13–C16–C20 of 17.7° and 15.7°, respectively, and metal–metal, intra-chain distances of 12.5 Å and 12.4 Å, respectively. Other selected structural features for **5** are presented in Tables 1 and 2.

When an equimolar, acetone–methanol solution of copper(II) hexafluoroacetylacetonate hydrate **6** and ditopic, bent dipyrindyl linker **7**, 2,5-bis(4-ethynyl-

pyridyl)furan, which is prepared via known literature procedures,<sup>1c</sup> is allowed to undergo slow evaporation, coordination polymer **8** results (Scheme 2).

As is the case with *N*-oxide polymers **3** and **5**, pyridyl-based polymer **8** exhibits one donor and one acceptor in its asymmetric unit (Fig. 3a). Also similar to **3** and **5**, a zig-zag chain is produced (Fig. 3b). In this instance, however, the shape results not from the hybridization present in the dative bond itself, but, instead, from the bite angle inherent to linker **7**. As a further consequence of utilizing nucleophilic tecton **7**, the polymer shows a “trough”-like form, with the upper edges defined by the furanyl rings (Fig. 3c). In this sense, **8** can also be viewed as a syndiotactic polymer, its furanyl moieties alternating from side to side of the “trough”. This interesting occurrence is derived from a combina-



Scheme 2

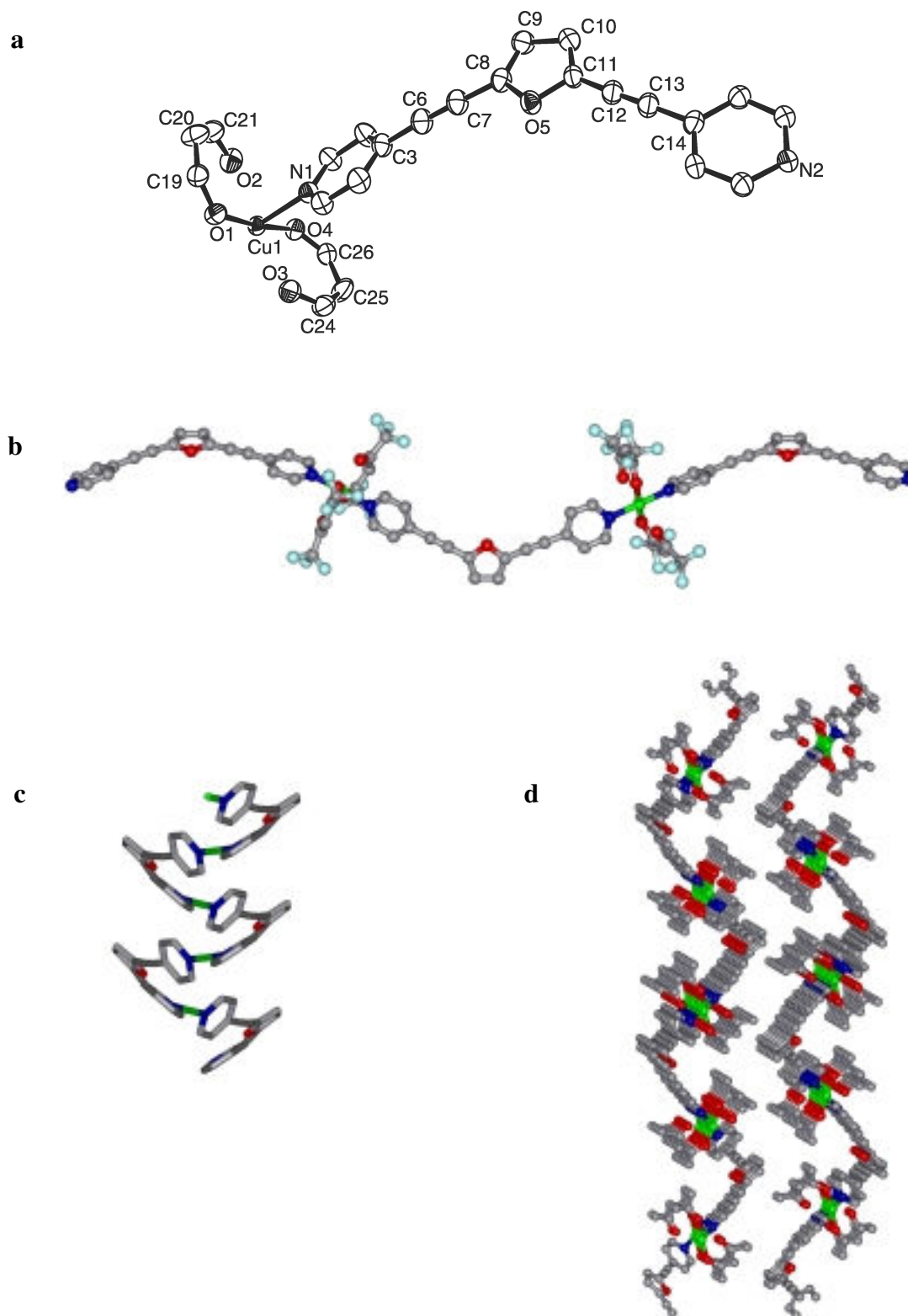


Fig. 3. (a) ORTEP plot of the asymmetric unit of **8** (protons and trifluoromethyl groups omitted for clarity). (b) Portion of the polymeric chain of **8** (ball and stick representation; protons omitted for clarity). (c) “Trough”-like shape taken by **8** (stick representation; protons and hfac groups omitted for clarity). (d) Stacking diagram of **8** (ball and stick representation; protons and fluorines omitted for clarity).

tion of crystal packing forces and the flexibility of **7**, with its two alkynyl groups extending its fundamental structure and making it “floppy”. The stacking diagram for **8** is as shown (Fig. 3d). Disorder, which has been deleted from Fig. 3, is seen in some of the trifluoromethyl groups’ fluorine atoms.

As is known for metal complex **6**,<sup>16</sup> a *trans*, 180° ligand arrangement about the pseudo-octahedral copper(II) center in **8** is realized. The copper–pyridyl bond lengths are also consistent with those reported in the literature (Cu1–N1 = 2.0 Å).<sup>16</sup> Polymers based on subunit **7** with zinc(II) complex **4** and a related species have been reported.<sup>1c</sup> In these cases, a mixture of *cis*, 90° and *trans*, 180° coordination motifs were observed, as were similar metal–pyridyl bond lengths (2.1–2.2 Å).

Structural parameters and selected details are represented in Tables 3 and 4, respectively.

When ditopic, pyridyl linker **7** is allowed to react with manganese(II) hexafluoroacetylacetonate trihydrate **1**, under conditions similar to those for the formation of **8**, but in the presence of benzene **9**, coordination polymer **10** is the result (Scheme 3).

The asymmetric unit of **10** contains one manganese acceptor **1**, one pyridyl donor **7**, and two enclathrated benzene molecules, one of which is at fifty percent occupancy (Fig. 4a). The benzene guests as well as the disorder seen for the trifluoromethyl groups’ fluorines have been omitted from Fig. 4.

Unlike **8**, the coordination about the metal center in **10** occurs in a *cis*, 90° fashion, yielding a helix instead

Table 3. Crystallographic parameters for compounds **8** and **10**

|  | <b>8</b>  | <b>10</b>   |
|--|---|---|
| formula  | C <sub>28</sub> H <sub>12</sub> CuF <sub>12</sub> N <sub>2</sub> O <sub>5</sub> | C <sub>37</sub> H <sub>21</sub> F <sub>12</sub> MnN <sub>2</sub> O <sub>5</sub> |
| <i>M</i>   | 747.94  | 856.50  |
| <i>T</i> /K                                      | 200(1)  | 200(1)  |
| system   | Monoclinic  | Monoclinic  |
| space group                                      | <i>P</i> 2 <sub>1</sub> / <i>c</i>  | <i>P</i> 2 <sub>1</sub> / <i>n</i>  |
| <i>a</i> /Å                                      | 7.59190(10)   | 10.9723(3)  |
| <i>b</i> /Å                                      | 20.6357(2)  | 24.4756(9)  |
| <i>c</i> /Å                                      | 19.4418(2)  | 14.3178(5)  |
| $\alpha$ /°                                      | 90  | 90  |
| $\beta$ /°                                       | 90.3150 (10)  | 93.7750(19)   |
| $\gamma$ /°                                      | 90  | 90  |
| <i>V</i> /Å <sup>3</sup>                         | 3045.79 (6)   | 3836.8(2)   |
| <i>Z</i>   | 4   | 4   |
| $\mu$ /mm <sup>-1</sup>                          | 0.831   | 0.446   |
| <i>R</i> 1 ( <i>I</i> > 2 $\sigma$ ( <i>I</i> )) | 0.0437  | 0.0635  |
| GOF  | 1.014   | 1.093   |

Table 4. Selected bond lengths [Å] and angles [°] for **8** and **10**

|                   | Compound <b>8</b> |            | Compound <b>10</b> |           |
|-------------------|-------------------|------------|--------------------|-----------|
| Bond lengths (Å)  | Cu(1)–O(1)        | 2.0746(15) | Mn(1)–O(4)         | 2.137(3)  |
|                   | Cu(1)–O(4)        | 2.0896(15) | Mn(1)–O(1)         | 2.153(3)  |
|                   | Cu(1)–O(2)        | 2.2141(15) | Mn(1)–O(2)         | 2.188(3)  |
|                   | Cu(1)–O(3)        | 2.2193(14) | Mn(1)–O(3)         | 2.195(3)  |
|                   | Cu(1)–N(1)        | 2.0028(15) | Mn(1)–N(1)         | 2.235(3)  |
|                   | Cu(1)–N(2)#1      | 2.0068(15) | Mn(1)–N(2)#1       | 2.240(3)  |
| Bond angles (deg) | O(1)–Cu(1)–O(2)   | 85.97(5)   | O(1)–Mn(1)–O(2)    | 81.00(11) |
|                   | O(4)–Cu(1)–O(3)   | 85.35(5)   | O(4)–Mn(1)–O(3)    | 82.13(11) |
|                   | N(1)–Cu(1)–N(2)#1 | 178.62(6)  | N(1)–Mn(1)–N(2)#1  | 92.63(12) |

Symmetry transformations used to generate equivalent atoms for **8**: #1 *x*+2, *-y*+1/2, *z*-1/2; #2 *x*-2, *-y*+1/2, *z*+1/2.

Symmetry transformations used to generate equivalent atoms for **10**: #1 *-x*-1/2, *y*-1/2, *-z*+1/2; #2 *-x*-1/2, *y*+1/2, *-z*+1/2 #3 *-x*, *-y*, *-z*.

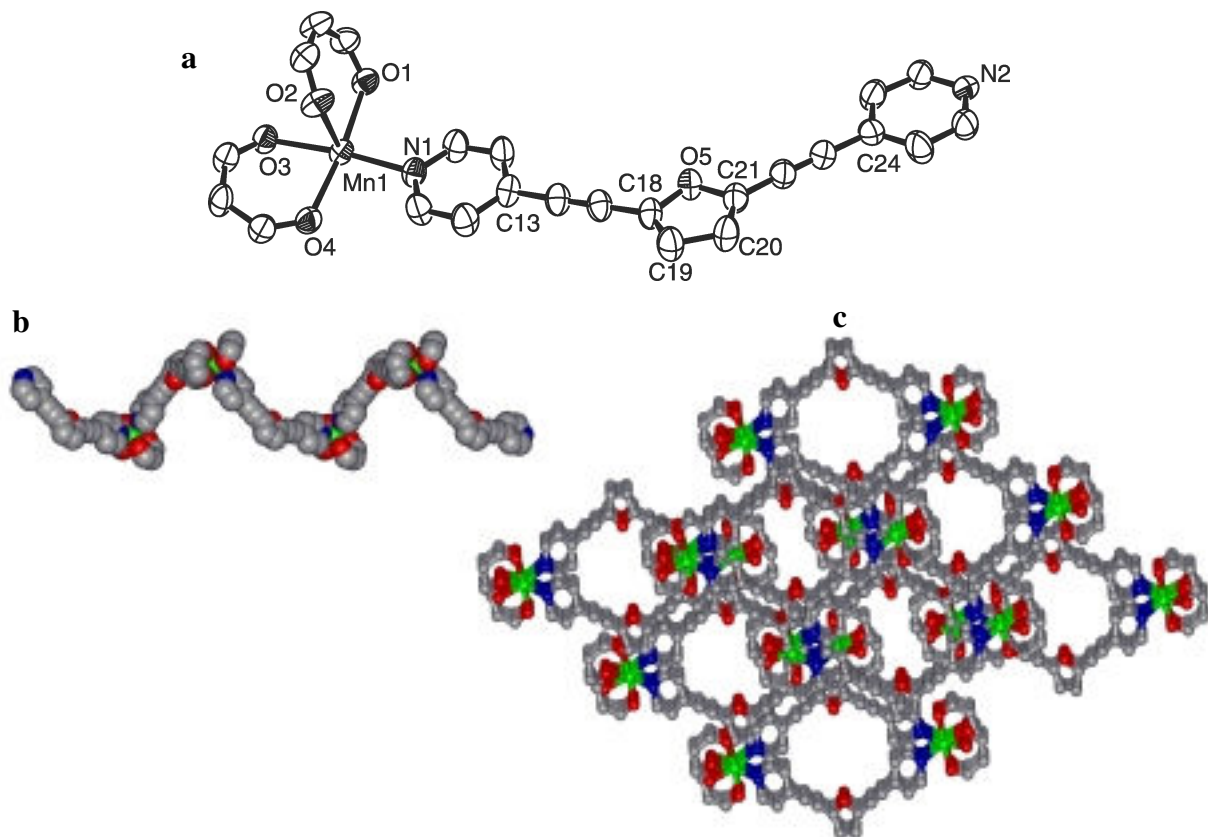
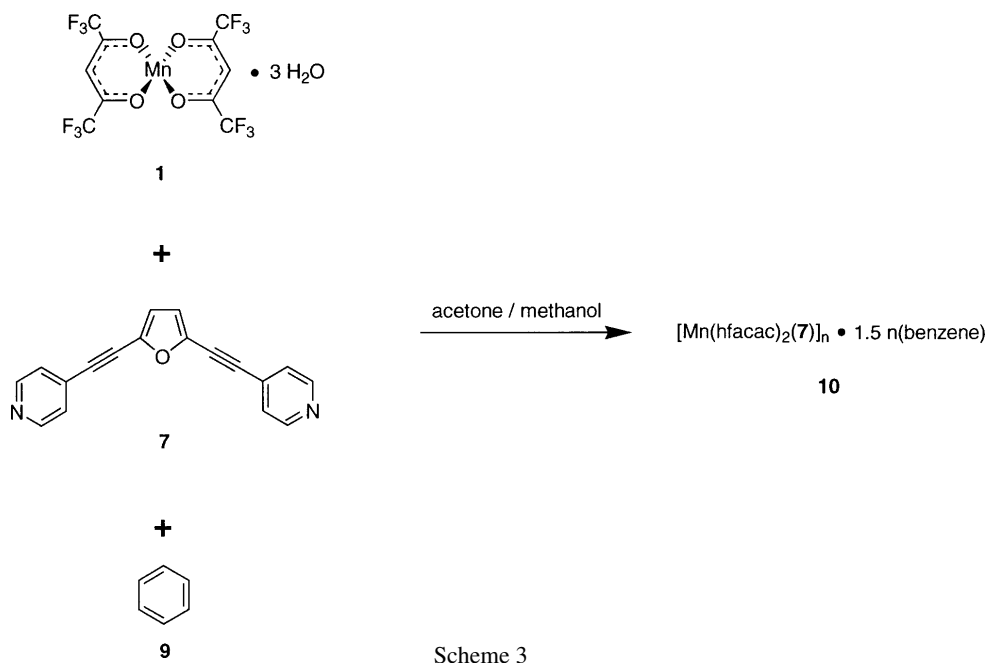
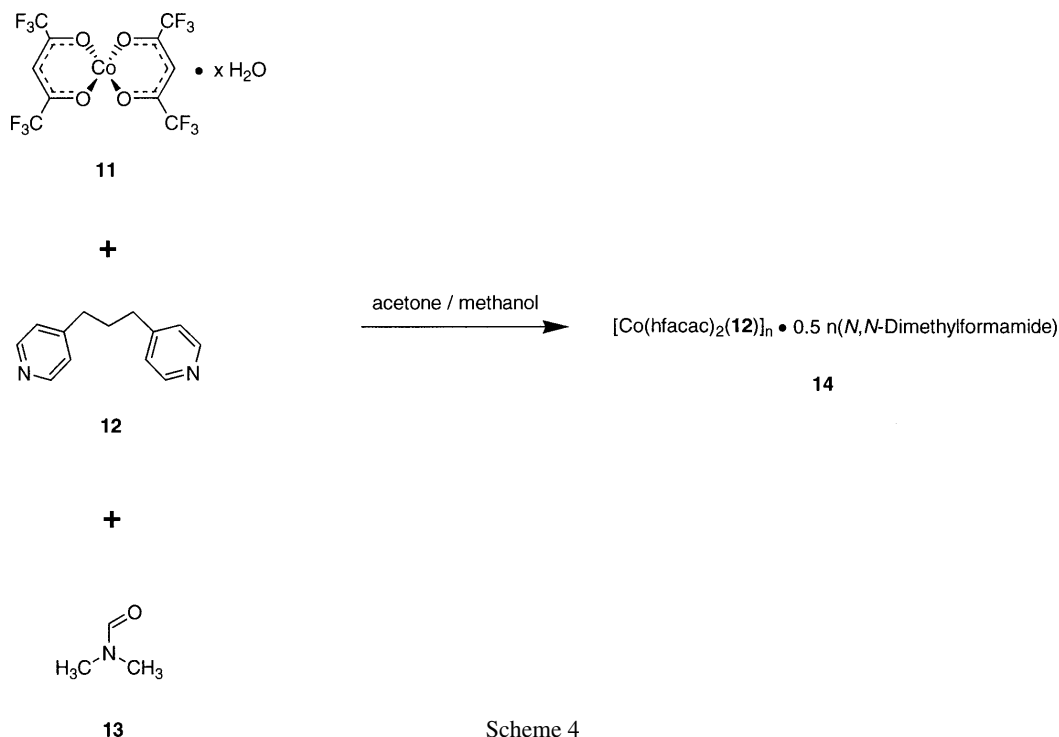


Fig. 4. (a) ORTEP plot of the asymmetric unit of **10** (protons, trifluoromethyl groups, and benzenes omitted for clarity). (b) Portion of the polymeric chain of **10** (CPK representation; protons, trifluoromethyl groups, and benzenes omitted for clarity). (c) Stacking diagram of **10** (ball and stick representation; protons, trifluoromethyl groups, and benzenes omitted for clarity).





Scheme 4

of a zig-zag chain (Fig. 4b). Having centrosymmetric space group  $P 2_1/n$ , an equivalent amount of *R*- and *S*-helices are present in any given crystal, rendering it optically inactive. The linear distance between every other manganese atom, which represents one full turn of the helix, is 24.5 Å. This value is significantly larger than those seen for similar helices based on subunit **1** and 4,4'-trimethylenedipyridine, where the vertical coil lengths ranged from 10.3 to 19.2 Å.<sup>9</sup> It is on the same order as a comparable helix constructed from zinc(II) building block **4** and linker **7** that has been reported (24.2 Å).<sup>1c</sup> The stacking seen for the crystal lattice of **10** is as shown (Fig. 4c).

The manganese–pyridyl bonds in **10** (2.24 Å) match those reported for other, analogous compounds in the literature (i.e., Mn–N(pyridyl) = 2.26 Å for the zig-zag chain that resulted from the reaction of **1** and 4,4'-dipyridyl).<sup>16</sup> Crystallographic parameters and selected structural details for **10** are presented in Tables 3 and 4, respectively.

Reacting cobalt(II) hexafluoroacetylacetonate hydrate **11** with 4,4'-trimethylenedipyridine **12** in an acetone–methanol solvent mixture and in the presence of *N,N*-dimethylformamide **13**, yields coordination polymer **14** in the solid state (Scheme 4).

The asymmetric unit of **14** consists of two independent ligand moieties **12**, two independent acceptor units **11**, and one enclathrated *N,N*-dimethylformamide mol-

ecule **13** (Fig. 5a). As is known in the literature, cobalt complexes similar to **11** undergo *trans* ligand coordination in reactions with pyridyl entities,<sup>19</sup> and this case is no exception. This gives the primary polymer chain of **14** an overall zig-zag form (Fig. 5b). Accounting for the discrepancy between the two independent metal-acceptor portions of **14**s asymmetric unit are the differing relative orientations for the trimethylene moiety of each inequivalent **12**. As per the common nomenclature,<sup>9,20</sup> carbons 39, 40, and 41 adopt a *TT* (*trans, trans*) configuration, while carbons 16 and 17 show a *trans* relationship and carbons 17 and 18 exhibit a *gauche* pattern, giving an overall *TG* configuration for carbons 16–18 (Fig. 5a). A similar, previously known compound based on copper(II) subunit **6** and the same, flexible dipyridyl unit **12** also gave a *trans* orientation about the metal center, but only a *TG* arrangement for the backbone of linker **12**.<sup>16</sup> Our previous, related work based on manganese(II) acceptor **1** and donor **12** resulted in multiple structures, depending on the organic template employed, but all exhibited a *cis* ligand coordination, and a variety of backbone configurations were observed.<sup>9</sup> The stacking diagram seen for **14** is as shown (Fig. 5c).

The cobalt–pyridyl bonds (2.11–2.16 Å) are on the order of those seen for similar compounds in the literature.<sup>19</sup> Structural parameters and selected details are represented in Tables 5 and 6, respectively.

When equimolar amounts of manganese(II) hexa-

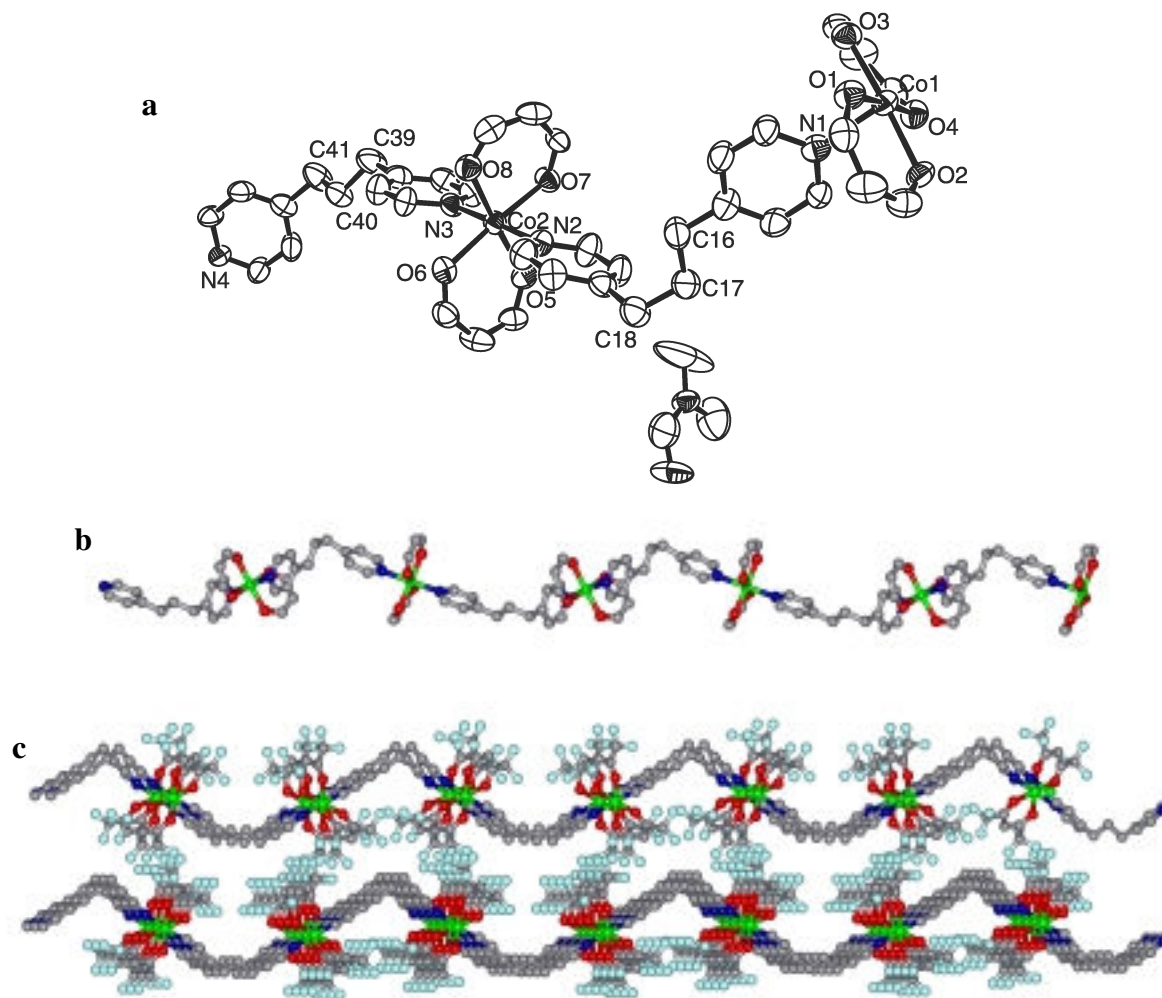


Fig. 5. (a) ORTEP plot of the asymmetric unit of **14** (protons and trifluoromethyl groups omitted for clarity). (b) Portion of the polymeric chain of **14** (ball and stick representation; protons, trifluoromethyl groups, and *N,N*-dimethylformamide molecules omitted for clarity). (c) Stacking diagram of **14** (ball and stick representation; protons and *N,N*-dimethylformamide molecules omitted for clarity).

fluoroacetylacetonate trihydrate **1** are reacted with *trans*-1-(2-pyridyl)-2-(4-pyridyl)-ethylene **15** in an acetone-methanol solution, the resulting solid state product is that of hydrogen-bonded coordination polymer **16** (Scheme 5).

The asymmetric unit of polymer **16** shows a total of two independent manganese atoms, each sitting on an inversion center, one linker **15**, one methanol molecule, and two independent hfacac moieties, whose disordered fluorine atoms have been omitted from the figure (Fig. 6a). This results in an interesting species that can be thought of as two metal complexes being hydrogen-bonded together to give a polymer with an overall zig-zag form (Fig. 6b). As is apparent, the first complex comprises two of donor **15** bound to one of metal accep-

tor **1** in a *trans* fashion, while the other consists of two methanol molecules connected, again in a *trans* arrangement, to a different subunit **1** through the oxygen atoms of their hydroxyl groups. It is the protons of these hydroxyl groups that form hydrogen bonds with the “free” 2-pyridyl ends of the first complex, bringing together the polymeric backbone ( $H1-N2 = 1.78 \text{ \AA}$ ). A known compound based upon metal building block **1** and a linker very similar to **15**, *trans*-1-(4-pyridyl)-2-(4-pyridyl)-ethylene, yielded an entirely different structure than that seen for **16**.<sup>17b</sup> In this case, both pyridyl groups of the donor ligand were bound to the manganese in a *cis* orientation, producing a generic zig-zag chain. It can be reasoned that the 2-pyridyl site is too sterically hindered

Table 5. Crystallographic parameters for compounds **14** and **16**

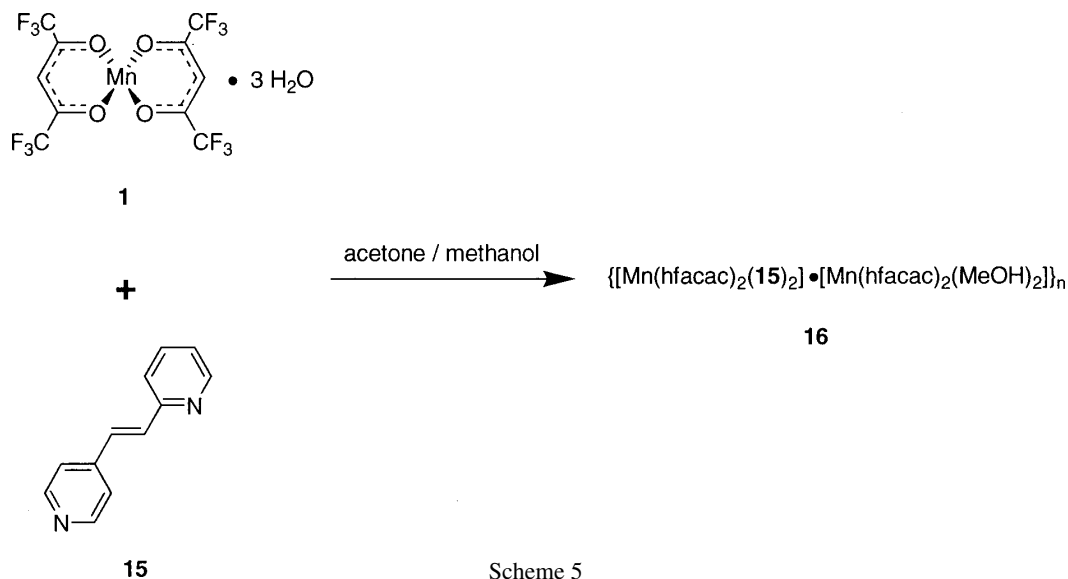
|   | <b>14</b>   | <b>16</b>   |
|---|---|---|
| formula   | C <sub>49</sub> H <sub>39</sub> Co <sub>2</sub> F <sub>24</sub> N <sub>5</sub> O <sub>9</sub> | C <sub>23</sub> H <sub>16</sub> F <sub>12</sub> MnN <sub>2</sub> O <sub>5</sub> |
| <i>M</i>  | 1415.71   | 683.32  |
| <i>T</i> /K                                     | 200(1)  | 200(1)  |
| system  | Triclinic   | Triclinic   |
| space group                                     | <i>P</i> 1  | <i>P</i> $\bar{1}$  |
| <i>a</i> /Å                                     | 7.6529(4)   | 9.0486(4)   |
| <i>b</i> /Å                                     | 9.5057(4)   | 9.5604(4)   |
| <i>c</i> /Å                                     | 20.0980(8)  | 16.6054(4)  |
| $\alpha$ /°                                     | 86.213(3)   | 76.220(2)   |
| $\beta$ /°                                      | 81.831(3)   | 82.146(2)   |
| $\gamma$ /°                                     | 88.887(3)   | 84.7183(15)   |
| <i>V</i> /Å <sup>3</sup>                        | 1443.98(11)   | 1379.42(9)  |
| <i>Z</i>  | 1   | 2   |
| $\mu$ /mm <sup>-1</sup>                         | 0.709   | 0.597   |
| <i>R</i> 1 ( <i>I</i> >2 $\sigma$ ( <i>I</i> )) | 0.0588  | 0.0474  |
| GOF   | 1.018   | 1.017   |

Table 6. Selected bond lengths [Å] and angles [°] for **14** and **16**

|                   | Compound <b>14</b> |          | Compound <b>16</b> |            |
|-------------------|--------------------|----------|--------------------|------------|
| Bond lengths (Å)  | Co(1)–N(1)         | 2.145(7) | Mn(1)–N(1)         | 2.295(2)   |
|                   | Co(1)–N(4)#1       | 2.113(6) | Mn(1)–N(1)#1       | 2.295(2)   |
|                   | Co(2)–N(3)         | 2.129(6) | Mn(2)–O(5)         | 2.1587(18) |
|                   | Co(2)–N(2)         | 2.156(6) | Mn(2)–O(5)#2       | 2.1587(18) |
| Bond angles (deg) | N(4)#1–Co(1)–N(1)  | 178.7(2) | N(1)–Mn(1)–N(1)#1  | 180.00(10) |
|                   | N(3)–Co(2)–N(2)    | 178.9(2) | O(5)#2–Mn(2)–O(5)  | 180.000(1) |

Symmetry transformations used to generate equivalent atoms for **14**: #1 *x*+2,*y*,*z*+1; #2 *x*-2,*y*,*z*-1.

Symmetry transformations used to generate equivalent atoms for **16**: #1 -*x*+2,-*y*+2,-*z*; #2 -*x*+1,-*y*+1,-*z*+1.



Scheme 5

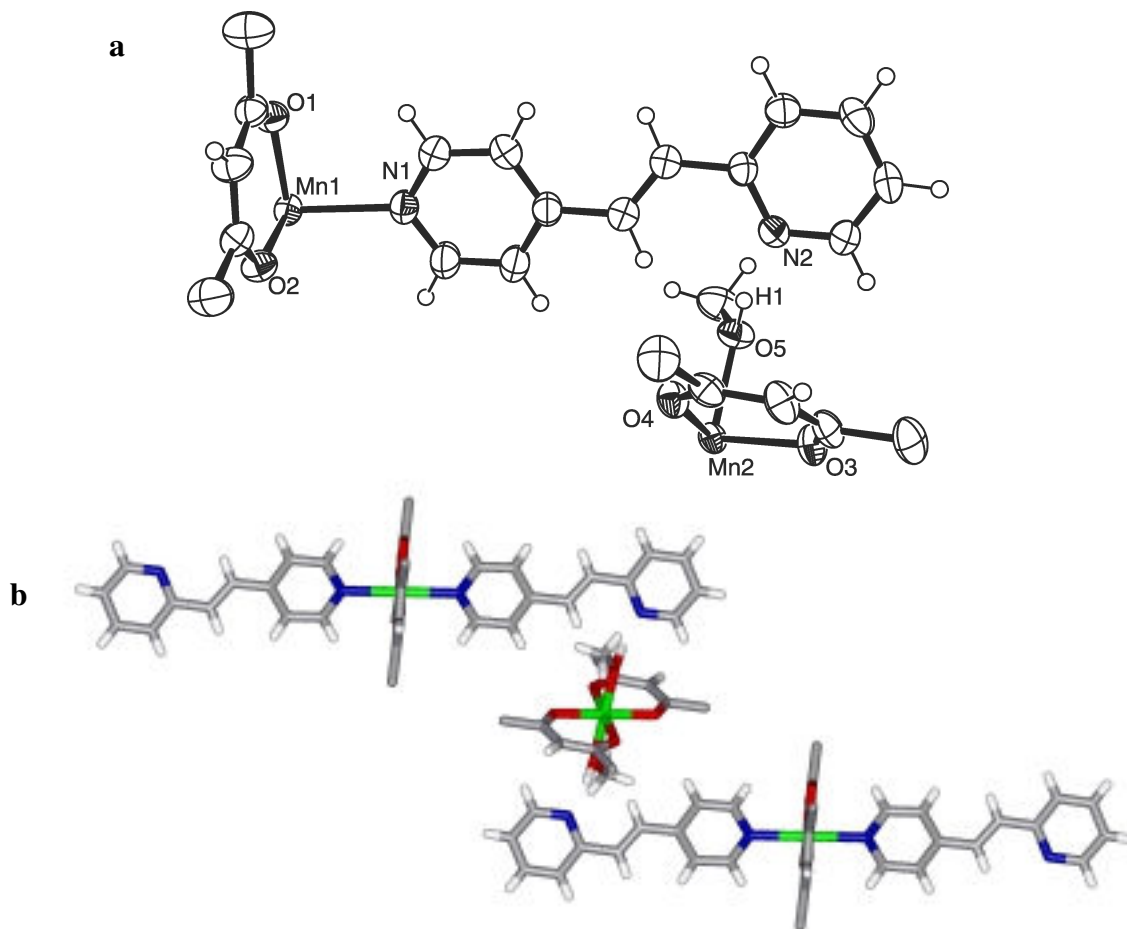


Fig. 6. (a) ORTEP plot of the asymmetric unit of **16** (fluorines omitted for clarity). (b) Portion of the polymeric chain of **16** (stick representation; fluorines omitted for clarity).

to allow for **15** to serve as a ditopic subunit, as its 4-pyridyl analogue did under similar reaction conditions. Taken on the whole, this result, along with our previous work in the field,<sup>9</sup> illustrates the interesting chemical and solid-state versatility of manganese(II) acceptor **1** under a variety of reaction conditions.

The manganese–nitrogen bond lengths for the pyridyl-bound complex ( $\text{Mn1–N1} = 2.30 \text{ \AA}$ ) in **16** are on the order of those found for the di-(4-pyridyl) counterpart reported in the literature ( $\text{Mn–N} = 2.26 \text{ \AA}$ ).<sup>17b</sup> Other selected structural features for **16** are presented in Tables 5 and 6.

### CONCLUSIONS

This work presents a continuation of our explorations into the solid-state structures of one-dimensional coordination polymers containing dipositive transition metal hexafluoroacetylacetonate (hfacac) complexes in their

backbones. In order to exploit, investigate, and probe a number of different bonding motifs, such as pyridyl–metal, pyridyl(*N*-oxide)–metal, and hydrogen bonding, a variety of donor subunits are utilized. The metal centers involved in this research are those containing manganese, zinc, copper, and cobalt, while the linkers binding them together are 4,4'-dipyridyl *N,N'*-dioxide hydrate **2**, 2,5-bis(4-ethynylpyridyl)furan **7**, 4,4'-trimethylenedipyridine **12**, and *trans*-1-(2-pyridyl)-2-(4-pyridyl)-ethylene **15**. A mixture of *cis* and *trans* ligand coordination is observed, depending on the individual circumstances of each reaction, and comparisons are made between the products themselves in addition to relevant compounds in the literature.

*Acknowledgments.* We thank the National Science Foundation for financial support of this research (CHE-9818472). We are also grateful to the A. v. Humboldt Foundation for a Feodor Lynen Fellowship for F. M. Tabellion.

## REFERENCES AND NOTES

- (1) (a) Bailar, J.C. In *Preparative Inorganic Reactions*, Vol. 1; Jolly, W.L., Ed.; Interscience: New York, 1964; pp 1–25. (b) Chen, C.-T.; Suslick, K.S. *Coord. Chem. Rev.* **1993**, *128*, 293–322 and references therein. (c) Ellis, W.W.; Schmitz, M.; Arif, A.M.; Stang, P.J. *Inorg. Chem.* **2000**, *39*, 2547–2557.
- (2) (a) Robson, R. In *Comprehensive Supramolecular Chemistry*, Vol. 6; Atwood, J.L.; Davies, J.E.D.; MacNicol, D.D.; Vögtle, F.; Lehn, J.-M., Eds.; Pergamon: Oxford, 1996; pp 733–755. (b) Goodgame, D.M.L.; Menzer, S.; Smith, A.M.; Williams, D.J. *J. Chem. Soc., Dalton Trans.* **1997**, 3213–3218. (c) Yaghi, O.M.; Davis, C.E.; Li, G.; Li, H. *J. Am. Chem. Soc.* **1997**, *119*, 2861–2868. (d) Zaworotko, M. *J. Chem. Soc. Rev.* **1994**, *23*, 283–288. (e) Hirsch, K.A.; Wilson, S.R.; Moore, J.S. *Chem. Eur. J.* **1997**, *3*, 765–771. (f) Robson, R. *J. Chem. Soc., Dalton Trans.* **2000**, 3735–3744. (g) Hagrman, P.J.; Hagrman, D.; Zubieta, J. *Angew. Chem., Int. Ed. Engl.* **1999**, *38*, 2638–2684. (h) Eddaoudi, M.; Moler, D.B.; Li, H.; Chen, B.; Reineke, T.M.; O’Keeffe, M.; Yaghi, O.M. *Acc. Chem. Res.* **2001**, *34*, 319–330.
- (3) (a) Lehn, J.-M. *Supramolecular Chemistry Concepts and Perspectives*; VCH: Weinheim, 1995; pp 139–160. (b) Swiegers, G.F.; Malefetse, T.J. *Chem. Rev.* **2000**, *100*, 3483–3537. (c) Chambron, J.-C.; Dietrich-Buchecker, C.; Sauvage, J.-P. In *Comprehensive Supramolecular Chemistry*, Vol. 9; Lehn, J.-M.; Atwood, J.L.; Davies, J.E.D.; MacNicol, D.D.; Vögtle, F., Eds.; Pergamon: Oxford, 1996; pp 43–83. (d) Caulder, D.L.; Raymond, K.N. *Acc. Chem. Res.* **1999**, *32*, 975–982. (e) Caulder, D.L.; Raymond, K.N. *J. Chem. Soc., Dalton Trans.* **1999**, 1185–1200. (f) Fujita, M. *Chem. Soc. Rev.* **1998**, *27*, 417–425. (g) Leininger, S.; Olenyuk, B.; Stang, P.J. *Chem. Rev.* **2000**, *100*, 853–908. (h) Saalfrank, R.W.; Uller, E.; Demleitner, B.; Bernt, I. In *Structure and Bonding*, Vol. 96; Fujita, M., Ed.; Springer: Berlin, 2000; pp 149–175.
- (4) (a) Inoue, M.; Kubo, M. *Coord. Chem. Rev.* **1976**, *21*, 1–27. (b) Hatfield, W.E.; Estes, W.E.; Marsh, W.E.; Pickens, M.W.; ter Haar, L.W.; Weller, R.R. In *Extended Linear Chain Compounds*, Vol. 3; Miller, J.S., Ed.; Plenum Press: New York, 1982; pp 43–142.
- (5) (a) Collman, J.P.; McDevitt, J.T.; Yee, G.T.; Leidner, C.R.; McCullough, L.G.; Little, W.A.; Torrance, J.B. *Proc. Natl. Acad. Sci. U.S.A.* **1986**, *83*, 4581–4585. (b) Collman, J.P.; McDevitt, J.T.; Leidner, C.R.; Yee, G.T.; Torrance, J.B.; Little, W.A. *J. Am. Chem. Soc.* **1987**, *109*, 4606–4614.
- (6) (a) Stucky, G.D.; Phillips, M.L.F.; Gier, T.E. *Chem. Mater.* **1989**, *1*, 492–509. (b) Belt, R.F.; Gashurov, G.; Liu, Y.S. *Laser Focus* **1985**, *21(10)*, 110–114.
- (7) Suslick, K.S.; Chen, C.-T. *Polym. Mater. Sci. Eng.* **1990**, *63*, 272–276.
- (8) (a) Braga, D.; Grepioni, F.; Desiraju, G.R. *Chem. Rev.* **1998**, *98*, 1375–1405. (b) Braga, D. *J. Chem. Soc., Dalton Trans.* **2000**, 3705–3713.
- (9) (a) Tabellion, F.M.; Seidel, S.R.; Arif, A.M.; Stang, P.J. *Angew. Chem., Int. Ed. Engl.* **2001**, *40*, 1529–1532. (b) Tabellion, F.M.; Seidel, S.R.; Arif, A.M.; Stang, P.J. *J. Am. Chem. Soc.* **2001**, *123*, 11982–11990.
- (10) COLLECT Data Collection Software. Nonius B.V., 1998. P.O. Box 811, 2600 AV Delft.
- (11) Otwinowski, Z.; Minor, W. *Methods Enzymol.* **1997**, *276*, 307–326.
- (12) SIR97 (Release 1.02)—A program for automatic solution and refinement of crystal structure. A. Altomare, M.C. Burla, M. Camalli, G. Cascarano, C. Giacovazzo, A. Guagliardi, A.G. G. Molteni, G. Polidori, and R. Spagna. Dipartimento Geomineralogica Campus Universitario, Via Orabona 4, 70125, Bari, Italy.
- (13) Sheldrick, G.M. SHELX97 [Includes SHELXS97, SHELXL97, CIFTAB], Programs for Crystal Structure Analysis (Release 97-2). University of Göttingen, Germany, 1997.
- (14) Maslen, E.N.; Fox, A.G.; O’Keefe, M.A. In *International Tables for Crystallography: Mathematical, Physical and Chemical Tables*, Vol. C; Wilson, A.J.C., Ed.; Kluwer, Dordrecht, The Netherlands, 1992; pp 476–516.
- (15) Creagh, D.C.; McDauley, W.J. In *International Tables for Crystallography: Mathematical, Physical and Chemical Tables*, Vol. C; Wilson, A.J.C., Ed.; Kluwer: Dordrecht, The Netherlands, 1992; pp 206–222.
- (16) Plater, M.J.; St. J. Foreman, M.R.; Slawin, A.M.Z. *Inorg. Chim. Acta* **2000**, *303*, 132–136.
- (17) For example: (a) Koga, N.; Ishimaru, Y.; Iwamura, H. *Angew. Chem., Int. Ed. Engl.* **1996**, *35*, 755–757. (b) Mago, G.; Hinago, M.; Miyasaka, H.; Matsumoto, N.; Okawa, H. *Inorg. Chim. Acta* **1997**, *254*, 145–150.
- (18) Complexes similar to **4** are known to occasionally adopt a *trans* orientation in interactions with pyridyl units (see ref 1c).
- (19) Elder, R.C. *Inorg. Chem.* **1968**, *7*, 1117–1123.
- (20) Carlucci, L.; Ciani, G.; v. Gudenberg, D.W.; Proserpio, D.M. *Inorg. Chem.* **1997**, *36*, 3812–3813.

